Received 27 May 2024; revised 8 July 2024 and 8 August 2024; accepted 9 August 2024. Date of publication 12 August 2024; date of current version 28 August 2024. The review of this article was arranged by Editor K. Cheng.

Digital Object Identifier 10.1109/JEDS.2024.3442474

Electrical Effect of Nitrogen Implanted Into LDD of MOSFETs

YOO SEON SONG, MARKUS LENSKI, MOHAMMED F. KARIM, KEITH FLYNN, JAN HOENTSCHEL, CARSTEN PETERS, JENS-UWE SACHSE, ÖMÜR IŞıL AYDIN, JUN WU, BASTIAN HAUßDÖRFER, MAHESH SIDDABATHULA, KONRAD SEMMLER, AND JÜRGEN DALEIDEN

Department of Process Integration, GlobalFoundries Dresden Module One LLC & Company, 01109 Dresden, Germany

CORRESPONDING AUTHORS: Y. S. SONG AND M. LENSKI (e-mail: yooseon.song@globalfoundries.com; markus.lenski@globalfoundries.com)

This work was supported in part by the European Union within "NextGeneration EU"; in part by the Federal Ministry for Economic Affairs and Climate Action (BMWK) based on a decision by the German Bundestag; and in part by the State of Saxony with Tax Revenues based on the Budget approved by the members of the Saxon State Parliament in the Framework of "Important Project of Common European Interest - Microelectronics and Communication Technologies", through the Project "EUROFOUNDRY."

ABSTRACT The motivation of this study was to solve the high $I_{D,off}$ problem in 8 Volt N-channel MOSFET. We experimented with implanting nitrogen into LDD at various doses. As a result, $I_{D,off}$ increases and BV_{DSS} decreases as the dose increases. When it exceeds 1.0E15 cm^{-2}, the occurrence of tail-type $I_{D,off}$ and BV_{DSS} that deviate from the normal distribution increases. Implanted nitrogen enhances the diffusion of dopants in the LDD bulk but suppresses it on the silicon surface. As a result, the depletion curvature at the LDD edge becomes a negative shape and increases the electric field. We performed the same experiment on logic MOSFETs to comprehensively analyze other electrical effects. Nitrogen improves the HCI immunity of MOSFETs but degrades for 2.5 Volt and 8 Volt MOSFETs when the dose is above 1.0E15 cm^{-2}. The short-channel effect of 2.5 Volt MOSFET is insensitive to nitrogen but is suppressed in CORE MOSFET when the dose is over 1.3E15 cm^{-2}. Nitrogen changes $I_{D,sat}$ through interactions with co-implanted species and nitrogen dose. As a result, nitrogen co-implanted with phosphorus shows a parabolic-like $I_{D,sat}$ trend. However, in the case of CORE MOSFET implanted with arsenic, $I_{D,sat}$ does not show a parabolic-like trend but increases continuously. This experiment did not find much benefit from nitrogen implantation for 2.5 Volt and 8 Volt MOSFETs. For all MOSFETs, it is recommended that the nitrogen dosage not exceed 1.0E15 cm^{-2}.

INDEX TERMS Arsenic, BV_{DSS}, DIBL, GIDL, $I_{D,off}$, $I_{D,sat}$, HCI, LDD, nitrogen, phosphorus.

I. INTRODUCTION

Planar CMOS semiconductors using nanometer technology are expanding their scope of application to display and embedded memory products. These products require MOSFETs that operate at higher voltages than the input/output MOSFETs (IO MOSFET). However, we observed occasionally high $I_{D,off}$ (source-drain leakage current at gate=0 Volt) problem in 8 Volt N-channel MOSFET (HV MOSFET). Optical Beam Induced Resistance Change (OBIRCH) analysis did not detect leakage current paths, and physical structural analysis revealed no clues. We suspected the nitrogen implantation into LDD as the root cause of the high $I_{D,off}$.

Nitrogen implantation is widely used in LDD today as it inhibits short-channel effects and improves HCI lifetime. Implanted nitrogen migrates quickly to the surface and forms a highly concentrated layer on the silicon surface during annealing. This piled-up nitrogen suppresses transient enhanced diffusion (TED) of dopants [1], [2]. It also effectively reduces the generation of fixed charges at the Si-SiO2 interface by Hot Carrier Injection (HCI) [2], [3]. Although such research has been actively conducted in submicron technology, additional research involving high-voltage MOSFET in nanometer technology is rare.

This study aims to verify whether nitrogen is responsible for the high $I_{D,off}$ and evaluate other electrical effects. For

this purpose, we experimented with nitrogen implanted into the LDD of the HV and 2.5 Volt IO MOSFETs with different doses, and the same experiment was also conducted on the 1.1 Volt CORE MOSFET for comprehensive analysis.

The results showed nitrogen was the root cause of high $I_{D,off}$ and low BV_{DSS}. We analyzed this mechanism by investigating the direction of dopant diffusion on the LDD surface and in the bulk through Cov (overlap capacitance between Gate and LDD) measurement and TCAD simulation. We also evaluated the short-channel effect and HCI performance as known to the benefit of nitrogen implantation. Although nitrogen is known to be an electrically inactive species, $I_{D,sat}$ response differently depending on the co-implanted species and nitrogen dose. We analyzed the mechanism from the perspective of channel length modulation and LDD resistance modulation.

II. EXPERIMENT

HV MOSFET received the Well implantation and a grown thick gate oxide film after completing the STI (Shallow Trench Isolation) module. After polysilicon gate patterning and spacer etching, HV MOSFET was coated with oxide and nitride films to protect it from subsequent fabrication processes. IO and CORE MOSFETs fabrication began with removing these protective films through masking and etching. Then, gate oxide films for CORE and IO MOSFETs were grown respectively, followed by polysilicon deposition and patterning. Finally, HV MOSFET protection films were removed, and all subsequent fabrication processes of HV MOSFET proceeded the same as those of IO MOSFET.

The HV and IO MOSFET experiment continued with opening the LDD window in the same mask, implanting phosphorus as a donor, and conducting nitrogen dose (N-dose) experiments. We implanted nitrogen with a dose ranging from 0 to 2.5E15 cm^{-2} at an energy of 8 KeV and conducted annealing. The annealing condition for these samples was N_2 environment at a temperature of 750°C for 30 minutes.

As for the N-dose experiment for CORE MOSFET, we opened another LDD window, implanted arsenic as a donor, and BF_2 with a high-degree tilt angle to prevent a short-channel effect. Then, implanted nitrogen under the same conditions as IO and HV MOSFETs. After completing the source and the drain implantation, samples were spike-annealed at 1050 °C. Finally, after the completion of the metallization layer, the electrical characteristics of the sample were measured. Figure 1 shows a schematic illustration of the three types of MOSFETs and their LDD implantation scheme used in the experiments.

III. RESULT AND DISCUSSION

A. EFFECT OF NITROGEN ON $I_{D,OFF}$, AND BV_{DSS}

The measured $I_{D,off}$ of HV MOSFET is shown in the boxplot in Figure 2. The X-axis is the N-dose and the Y-axis is $I_{D,off}$. As N-dose increases, the median of $I_{D,off}$ increases, and the occurrence of tail-type $I_{D,off}$ that deviate from the normal distribution increases when it exceeds 1.0E15 cm^{-2}.

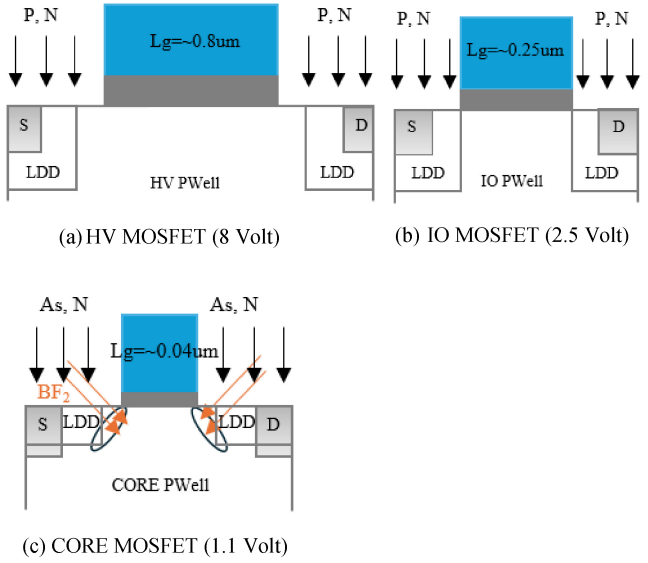

FIGURE 1. Schematic illustration of MOSFETs and LDD implantation. Lg: Gate length, S: Source, D: Drain.

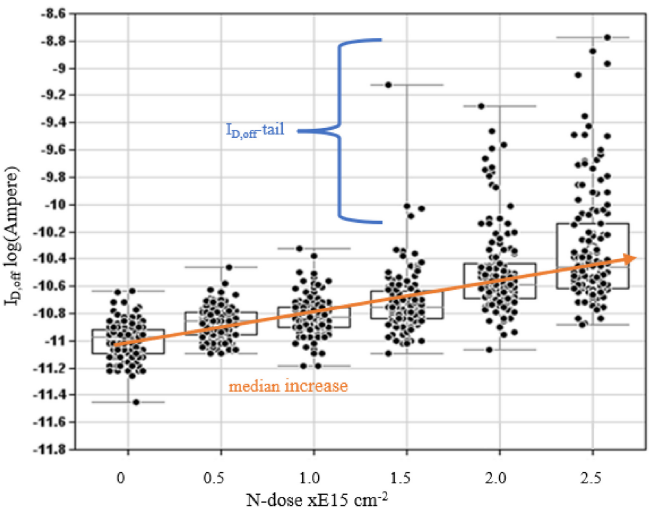

FIGURE 2. The $I_{D,off}$ trend of HV MOSFETs shows an increase in median and tail-type as N-dose increases. Read at V_D=8 Volt, V_S=V_G=V_B=0 Volt.

A.1. INCREASE IN $I_{D,OFF}$

Typically, $I_{D,off}$ increases due to DIBL (Drain-Induced Barrier Lowering) or GIDL (Gate-Induced Drain Leakage). DIBL is a barrier lowering as the drain voltage increases in short-channel MOSFET. Therefore, the drain current (I_D) curve moves upward in the subthreshold characteristics, decreasing $V_{T,sat}$ (threshold voltage measured at V_D=V_{DD}), and increasing $I_{D,off}$. GIDL is the tunneling current increased by an electric field. This occurs at the junction between the drain and accumulation layer below the gate when the gate voltage (V_G) approaches 0 Volt at high drain voltage (V_D) [4].

The upper curves in the subthreshold characteristics are measured at V_D of 8 Volt and the middles are at 5 Volt. The bottoms are measured in the linear region at V_D of 0.1 Volt

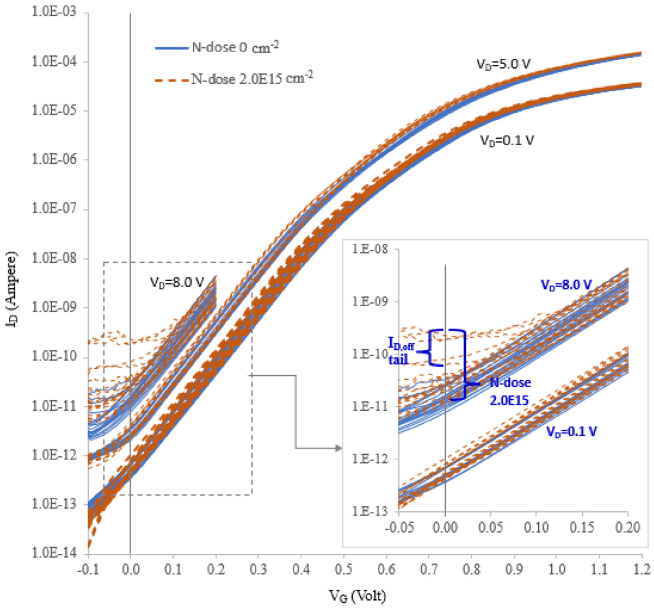

FIGURE 3. Subthreshold curve comparison between N-dose of 2.0E15 cm^{-2} and without nitrogen implantation (N-dose 0) for HV MOSFET. Sweep V_G, at V_D=0.1, 5, and 8 Volt, V_S=V_B=0 Volt.

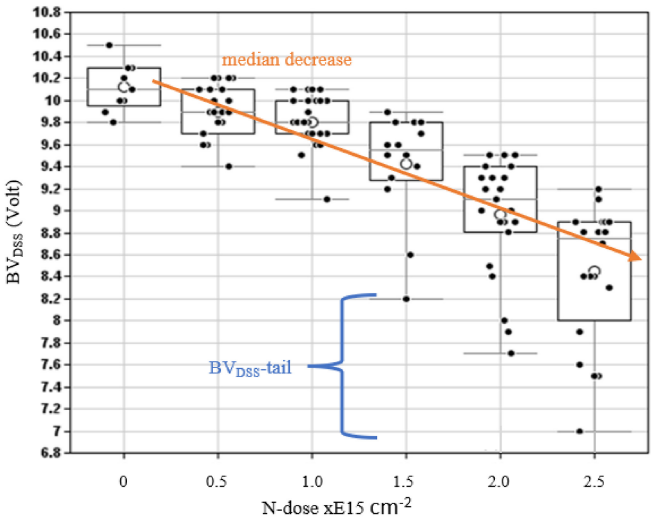

FIGURE 4. BV_{DSS} of HV MOSFETs shows a decreasing trend in the median and tail-type as N-dose increases. Read at I_D=0.1nanoAmpere (nA), sweep V_D, V_S=V_G=V_B=0 Volt.

(Fig. 3). If nitrogen implantation is responsible for DIBL, the I_D curves for the N-dose 2.0E15 cm^{-2} measured at 8 Volt or 5 Volt should shift above the curves for the N-dose of 0. However, most curves overlap with N-dose 0. Thus the high $I_{D,off}$ is not a result of DIBL.

We zoomed in on the I_D curves for V_D of 8 Volt around the V_G=0 Volt. These curves shift slightly upward at V_G=0 Volt compared to N-dose 0, but a few curves show abnormally high I_D with showing GIDL. These curves were measured on the $I_{D,off}$-tail MOSFETs. This result indicates that the implanted nitrogen increases the electric field. In the following, we evaluated whether this GIDL is a subthreshold leakage current due to the tunneling effect or comes from the breakdown voltage drop.

A.2. INCREASE IN BV_{DSS}

We measured BV_{DSS} and plotted it as a boxplot in Figure 4. The median of BV_{DSS} decreases as N-dose increases, and when N-dose exceeds 1.0E15 cm^{-2}, tail-type BV_{DSS} that deviate from the normal distribution increases. These results indicate that high $I_{D,off}$ is caused by the same mechanism as the low BV_{DSS}.

Breakdown is the phenomenon of significant current flow when the reverse bias reaches the threshold voltage. There are two breakdown mechanisms, that is punch-through and avalanche breakdown. Punch-through breakdown typically occurs in low-channel doping or short-channel MOSFET. It begins with injecting source carriers into the depletion of the drain when it approaches source depletion [4]. Avalanche breakdown occurs by producing multiplicative electron-hole pairs when hot electrons that gain kinetic energy from an electric field collide with the lattice [5].

To verify whether the BV_{DSS} mechanism in HV MOSFET is a punch-through or avalanche breakdown, we compared the I-V curve of BV_{DSS} with that of BV_{DBO} for gate length ~0.8 μm and ~10 μm MOSFETs (Fig. 5). The gate length of ~10 μm is the reference for avalanche breakdown because it is long enough that punch-through breakdown is unlikely. BV_{DBO} is an open terminal of gate and source, thus the source carriers cannot be injected into the drain even when the drain depletion reaches the source depletion. Therefore, the breakdown mechanism of BV_{DBO} is an avalanche breakdown [6]. If BV_{DSS} shows a lower voltage than BV_{DBO}, the BV_{DSS} should be punch-through. Otherwise, it's an avalanche breakdown. Figure 5 is a comparison of breakdown I-V curves between BV_{DSS} and BV_{DBO}. The X-axis is a V_D, and the Y-axis is an I_D. BV_{DSS} of ~0.8 μm MOSFET shows a slightly lower voltage than BV_{DBO}, but the offset is comparable to ~10 μm. Thus, the breakdown mechanism of BV_{DSS} is an avalanche. This result indicates that the implanted nitrogen increases the electric field and as a result, BV_{DSS} decreases.

A.3. DISCUSSION OF INCREASING ELECTRIC FIELD

In planar semiconductor fabrication, implanted dopants in an open window diffuse into vertical and lateral directions. As a result, a parallel-plane junction is formed at the bottom of the window and a curvature junction is formed at the edge. Unlike the bottom, the electric field is crowded at the curvature, and the electric field increases. As a result, the avalanche breakdown occurs at the junction edge. Therefore, to obtain a high breakdown voltage, the radius of curvature must be increased by deepening the junction depth [7].

According to the literature, phosphorus co-implanted with nitrogen enhances the TED of the dopant, increasing the junction depth by approximately two orders in bulk [8]. We obtained the same results as the literature through

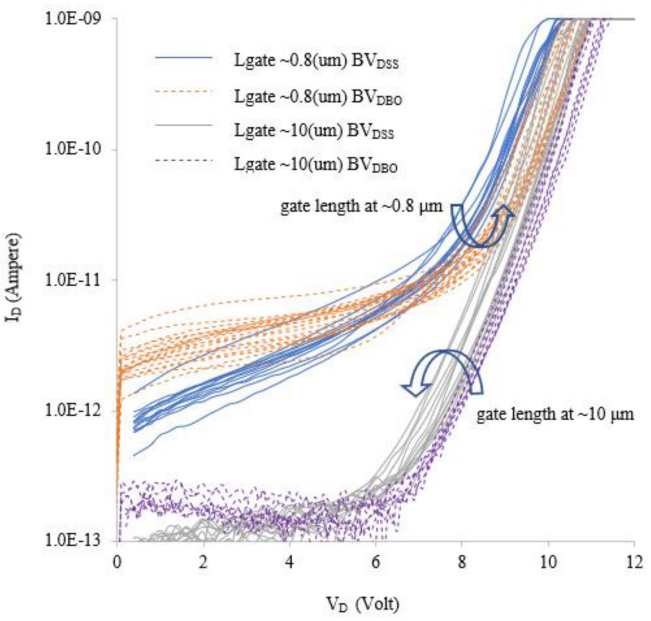

FIGURE 5. **BV_{DSS} of HV MOSFETs is comparable to BV_{DBO} for the gate lengths of ~0.8 μm and ~10 μm. BV_{DSS} sweep V_D at V_S=V_G=V_B=0 Volt and BV_{DBO} sweep V_D at V_B=0 Volt, V_S=V_G=open.**

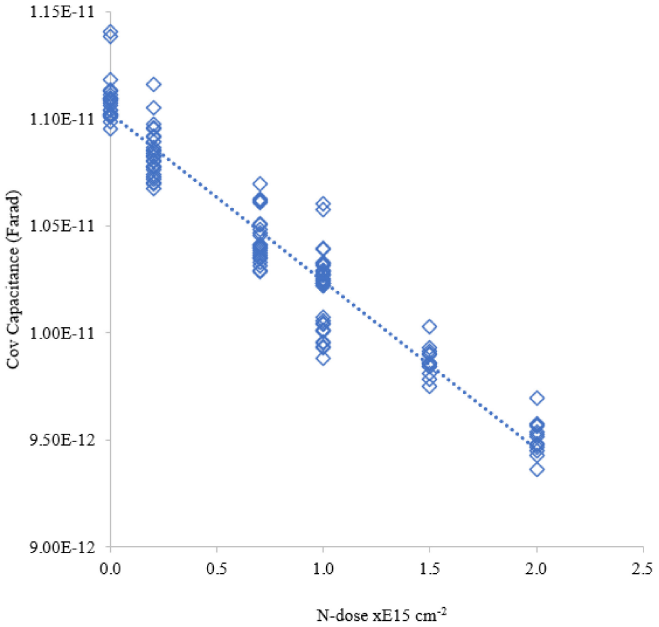

FIGURE 7. **Cov decreases linearly with increasing N-dose. This indicates that implanted nitrogen inhibits lateral diffusion of LDD.**

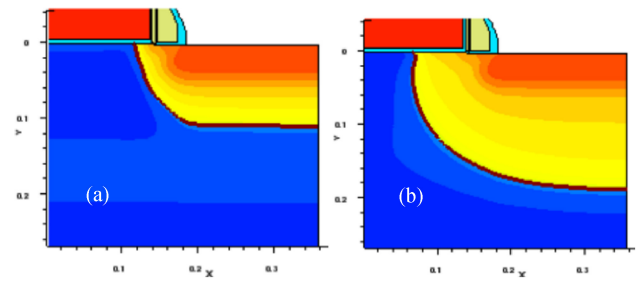

FIGURE 6. **LDD junction of IO MOSFET simulated by TCAD. N-dose of 1.0E15 cm^{-2} (b) shows deeper junction and curvature than without nitrogen implantation (a).**

TCAD simulations. The TCAD Deck was calibrated with Secondary Ion Mass Spectrometry (SIMS) data measured after co-implanting phosphorus and nitrogen into a wafer and annealing it. Figure 6 shows a simulated cross-section of the LDD junction of IO MOSFET shared with HV MOSFET. (a) is without nitrogen implantation and (b) is with nitrogen of 1.0E15 cm^{-2}. (b) shows a deeper LDD junction with a larger radius curvature and bigger overlaps to the gate than (a). According to the breakdown mechanism and TCAD results, BV_{DSS} should increase as N-dose increases, but the experiment shows the opposite result.

To analyze this discrepancy, we measured Cov representing the relative distance of the LDD diffusion under the gate. Figure 7 shows Cov on the Y-axis as a function of N-dose on the X-axis. It decreases linearly with a negative correlation coefficient for N-dose. This indicates that nitrogen inhibits the lateral diffusion of LDD under the gate.

We investigated the behavior of dopant diffusion on the surface. According to the literature, implanted nitrogen migrates quickly to the silicon surface during annealing, forming a high-concentration layer exceeding ~1E21 cm^{-3}. However, this concentration drops sharply as it is deeper from the surface, and approximately 75% of the nitrogen atoms are present at a depth of 20 Å [9]. This shallow and high-concentration nitrogen layer suppresses the TED of phosphorus on the silicon surface and reduces Cov.

In this way, phosphorus diffuses in opposite directions in the bulk and on the surface. It changes the depletion curvature at the LDD edge to a negative shape, i.e., moving outward of the channel on the surface and inward in the bulk. Therefore, the depletion curvature under the gate induces a strong electric field. As a result, GIDL occurs and BV_{DSS} drops as N-dose increases. The depletion curvature shape of the LDD edge illustrated in Figure 8 is similar to the depletion curvature of the GIDL.

A.4. DISCUSSION OF TAIL-TYPE $I_{D,OFF}$ AND BV_{DSS}

We observed that occurrences of tail-type $I_{D,off}$ and BV_{DSS} increased when N-dose exceeded 1.0E15 cm^{-2}. The $I_{D,off}$ measured on N-dose of 2.5E15 cm^{-2} was recorded in log(Ampere) at the same coordinates in Figure 9. Among them, $I_{D,off}$ greater than −10.1 log(Ampere) was defined as $I_{D,off}$-tail and marked in red, and other segments were marked in green. The red segments are distributed randomly within and between wafers.

We compared the breakdown characteristics of BV_{DSS} with N-dose of 2.5E15 cm^{-2} and 0.5E15 cm^{-2} in Figure 10. The I-V curves of N-dose 2.5E15 cm^{-2} are divided into two groups. One is the red-dash curves measured on the red segments, and another is the red-bold curves measured on the green segments.

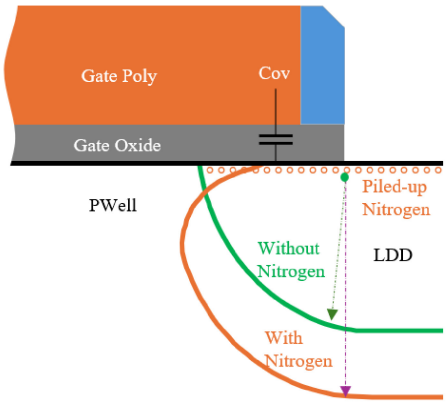

FIGURE 8. The depletion curvature at the edge of the LDD exhibits a negative curve because nitrogen suppresses lateral diffusion on the surface and enhances TED diffusion in the LDD bulk.

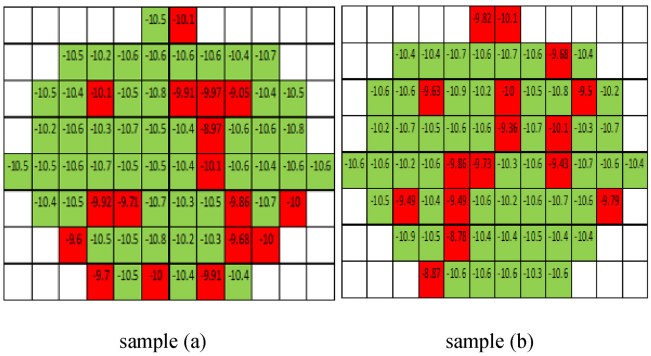

FIGURE 9. Red segments are $I_{D,off}$-tails of HV MOSFETs randomly distributed within and between wafers. Gate length = ~0.8 μm, N-dose 2.5E15 cm^{-2}.

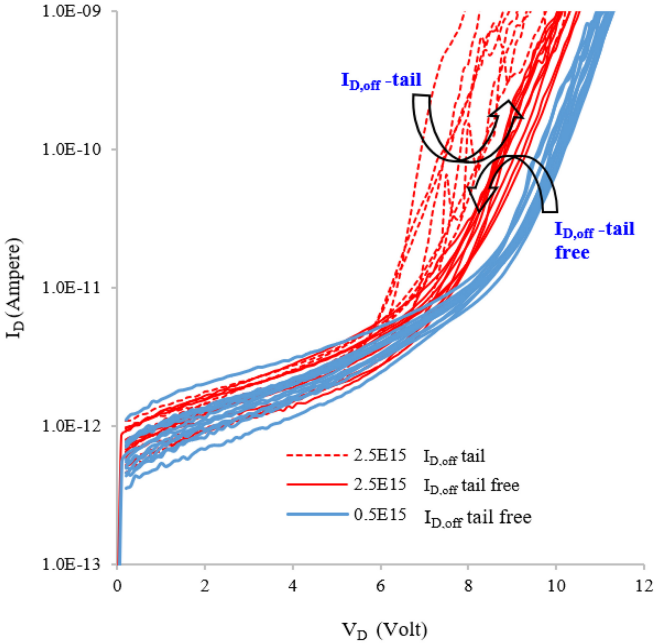

FIGURE 10. BV_{DSS} of HV MOSFETs for N-dose 2.5E15 cm^{-2} and 0.5E15 cm^{-2}. Gate length = ~0.8 μm.

The measured curves at 0.5E15 cm^{-2}, where $I_{D,off}$-tail is free, are shown as bold-blue curves. The red-bold curves show a similar variability but a lower breakdown voltage than the blue-bold ones. However, the red-dash curves have bigger variability and lower breakdown voltage than the red-bold ones. The coexistence of low breakdown voltage with high variation on the same wafer implies the presence of strong and random electric fields. The possible causes are the non-uniform dopant diffusion or doping concentrations. In the nanometer technology, random dopant fluctuation (RDF) was reported as increasing electric variability [10]. However, such reports are rare in the submicron gate length MOSFET.

Typically, dopants implanted into single-crystal silicon diffuse uniformly during thermal processes. However, the diffusivity of dopants in the amorphous silicon is slower than in single crystals [11]. Therefore, amorphous clusters generate steeper junctions and form stronger electric fields than single crystals. We investigated the presence of amorphous clusters due to nitrogen implantation.

The implanted nitrogen atoms migrate to the silicon surface during the annealing and most of them disappear from the implanted bulk silicon. However, if the thermal budget is insufficient or the dose is too high, the nitrogen solubility at the silicon surface will quickly saturate and migration to the surface will stop. Then, nitrogen atoms remain in the bulk silicon and increase the nitrogen concentration. These nitrogen atoms in the bulk retard the recrystallization of damaged silicon during implantation. As a result, amorphous clusters remain in LDD [12]. According to the literature, samples with N-dose 7E14 cm^{-2} and 2E15 cm^{-2} were annealed at 750 °C for 2 minutes and analyzed for crystal domain formation by Transmission Electron Microscopy (TEM). The result shows that 7E14 cm^{-2} was completely recrystallized, and the amorphous clusters disappeared. However, 2.0E15 cm^{-2} still shows the amorphous clusters that have not recrystallized [12]. Therefore, high-dose nitrogen implantation leaves amorphous clusters, resulting in randomly steep junctions. As a result, a strong electric field is generated at the amorphous clusters, which increases the occurrence of $I_{D,off}$-tail and BV_{DSS}-tail.

In the subthreshold characteristics discussion, GIDL was observed in MOSFETs where $I_{D,off}$-tails occurred. We investigated the breakdown I-V characteristics to verify whether the cause of the GIDL was the breakdown voltage reduction or an increase in subthreshold leakage current. In Figure 10, the I-V curves of 0.5E15 cm^{-2} are before the breakdown at V_D of 8 Volt, but the red-dash curves of 2.5E15 cm^{-2} are already in the breakdown and have significant current flow. Therefore, the cause of the GIDL observed in $I_{D,off}$-tail MOSFETs is not the subthreshold leakage current due to the tunneling effect, but the breakdown voltage drop.

B. NITROGEN EFFECT ON HCI DEGRADATION

We observed that implanted nitrogen increases the electric field. This suggests nitrogen implantation may reduce HCI

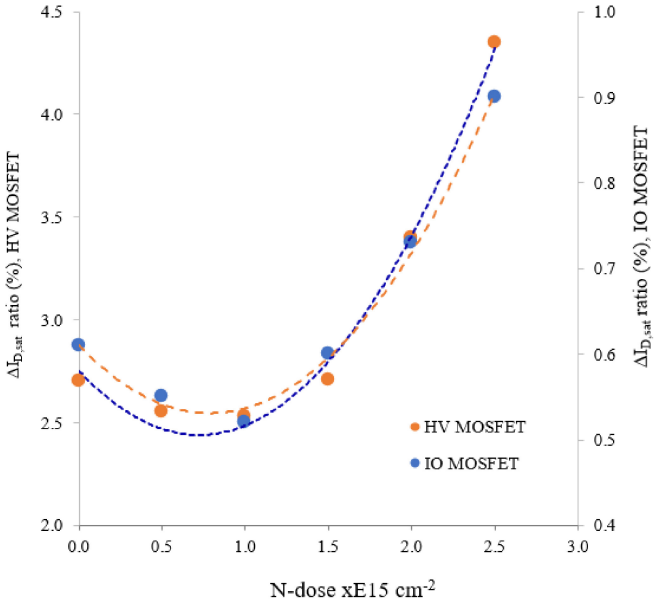

FIGURE 11. fWLR of HV MOSFET (Y1) and IO MOSFET (Y2), lower $\Delta I_{D,sat}$ is better for HCI immunity. V_D=5.5 Volt, V_G=I_{BMAX}, for 100 seconds.

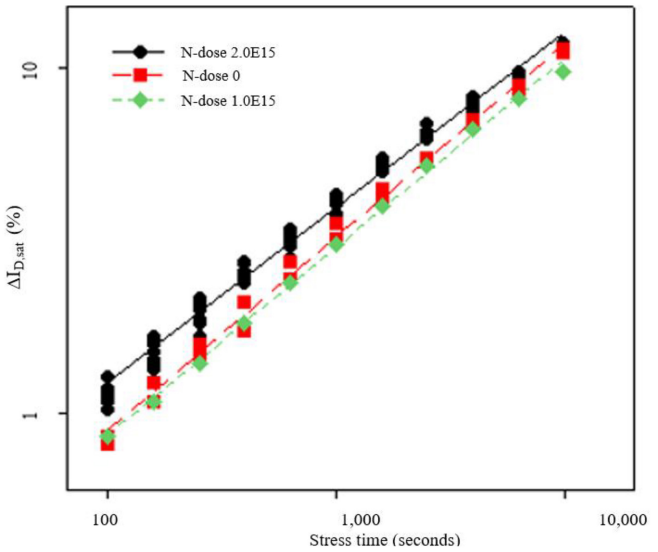

FIGURE 12. HCI test on IO MOSFETs for 10,000 seconds stress time for N-dose 0, 1.0E15, 2.0E15 cm^{-2}. V_D=3.6 Volt, V_G=I_{BMAX}.

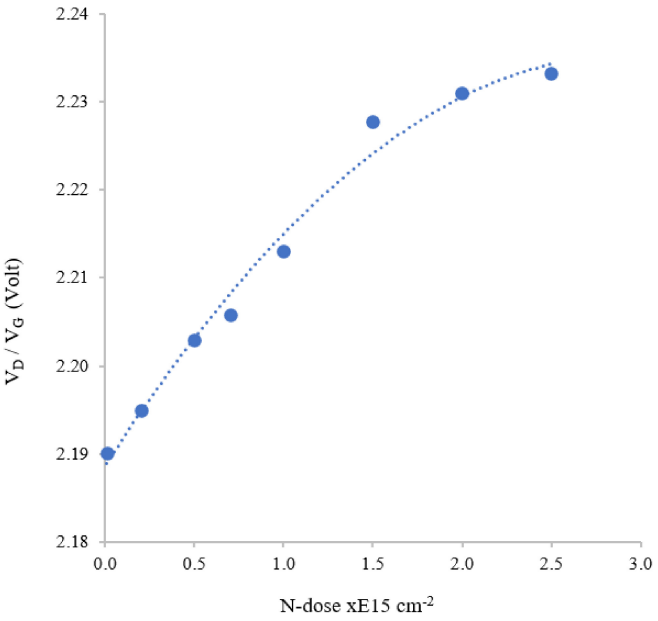

FIGURE 13. fWLR of CORE MOSFET, higher V_D/V_G is better for HCI immunity. Ramping V_D=V_G=0.002 Volt per second.

immunity by providing stronger kinetic energy to the hot electrons [13]. To verify the HCI degradation due to nitrogen implantation, we measured it with the fWLR (Fast Wafer Level Reliability). This is an effective method for measuring many samples and understanding the trend for N-dose. However, it is a relative measurement for a short stress time. Therefore, we tested HCI degradation for 10,000 seconds of stress on a few selected samples to verify the fWLR results.

B.1. TREND OF HCI DEGRADATION FOR N-DOSE

fWLR measurement is reported as $\Delta I_{D,sat}$ which is the percent of $I_{D,sat}$ shift ratio from the initial to the 100 seconds stress time. Figure 11 shows the $\Delta I_{D,sat}$ of HV MOSFET on the Y1-axis and IO MOSFET on the Y2-axis. Both show similar trends, that is $\Delta I_{D,sat}$ decreases as increases in N-dose until 1.0E15 cm^{-2}. However, they show inflection points at 1.0E15 cm^{-2} and rise sharply after passing them. This means the HCI immunity is enhanced by nitrogen implantation, but this effect disappears at 1.0E15 cm^{-2} and begins to degrade.

To confirm the HCI degradation trend observed in fWLR, HCI testing was performed on the IO MOSFET for 10,000 seconds for N-doses of 0, 1.0E15, and 2.0E15 cm^{-2}. Figure 12 shows the stress time on the X-axis and $\Delta I_{D,sat}$ on the Y-axis. Among these MOSFETs, the $\Delta I_{D,sat}$ measured at N-dose 1.0E15 cm^{-2} consistently shows the lowest shift ratio up to 10,000 seconds, and the highest shift ratio observed at the highest dose of 2.5E15 cm^{-2}. The sample without nitrogen implantation shows intermediate. These results are consistent with fWLR results.

We measured the HCI degradation of CORE MOSFET using the fWLR to verify the observation of inflection points in IO and HV MOSFETs. This result is reported as V_D and V_G (V_D/V_G) voltage at which the $\Delta I_{D,sat}$ reaches 5%. Therefore, higher V_D/V_G indicates improving HCI immunity, but it is opposite to $\Delta I_{D,sat}$ in IO and HV MOSFETs. fWLR results in Figure 13 show that the HCI immunity improves without an inflection point even as the N-dose increases to 2.5E15 cm^{-2}.

We performed HCI testing for 10,000 seconds for 0.2E15, 0.7E15, and 1.5E15 cm^{-2} to confirm the fWLR result of CORE MOSFET. Figure 14 shows the HCI testing results for 10,000 seconds of stress time. Higher N-dose consistently maintains a lower $\Delta I_{D,sat}$ trend from 100 seconds to 10,000 seconds like the fWLR results.

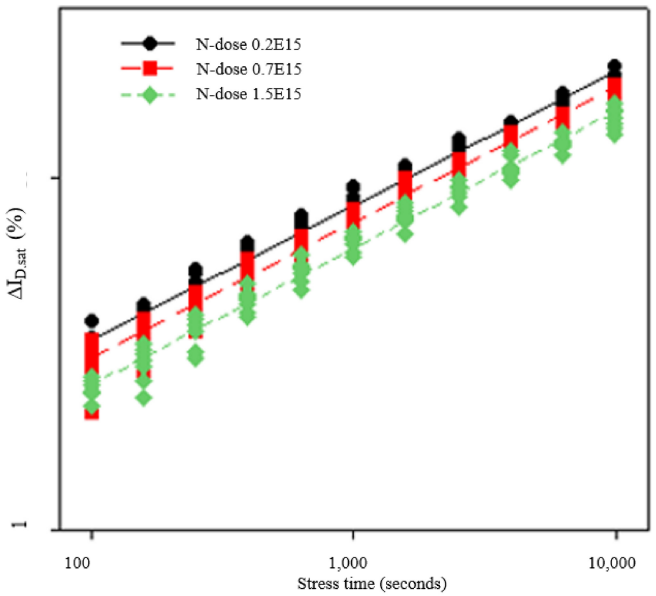

FIGURE 14. HCI test on CORE MOSFETs for 10,000 seconds stress time for N-dose 0.2E15, 0.7E15, and 1.5E15 cm^{-2}. V_D=V_G=1.7 Volt.

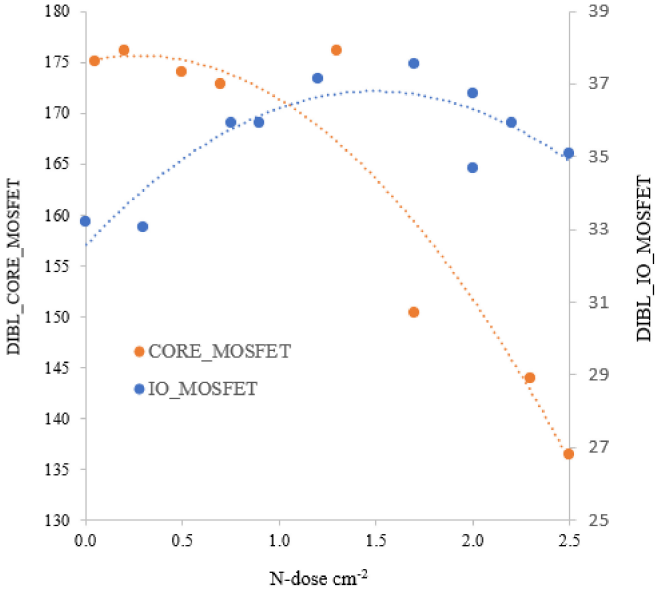

FIGURE 15. IO MOSFET (Y2) does not respond to N-dose, but CORE MOSFET (Y1) shows a DIBL drop at N-dose above 1.3E15 cm^{-2}.

B.2. DISCUSSION OF NITROGEN EFFECT ON HCL DEGRADATION

We observed that the HCI immunity improved up to 1.0E15 cm^{-2} for HV and IO MOSFETs and continued to improve up to 2.5E15 cm^{-2} for CORE MOSFETs. This is because of the formation of a high-concentrated nitrogen layer on the silicon surface [2], [3], [9]. Hot electrons leaving at the edge of the LDD receive kinetic energy from the electric field in the depletion layer. They collide with the gate oxide and create a fixed charge at the Si-SiO2 interface. However, the high-concentration nitrogen layer reduces the impact of collision and suppresses the generation of fixed charges. As a result, increasing N-dose improves HCI immunity [2], [3].

However, we observed the HCI degradation in IO and HV MOSFETs when the N-dose exceeds 1.0E15 cm^{-2}. A possible root cause is an increase in the electric field. In Section III.A, we observed the electric field. Therefore, a higher N-dose provides stronger kinetic energy to the hot electrons and creates more fixed charges. HCl degradation begins with the N-dose of 1.0E15 cm^{-2}. This indicates that the suppression of HCl degradation by the high-concentration nitrogen layer is dominated by the effect of increasing the electric field as N-dose increases. The possible reason for such HCI degradation only occurring in IO and HV MOSFETs is that they have a higher operating voltage than CORE MOSFET or the LDD junction profile is different.

C. SHORT CHANNEL EFFECT

Nitrogen implanted into LDD is known to suppress the short-channel effect [1]. This is one of the reasons why nitrogen implantation is widely used today. We analyzed the DIBL to verify the short-channel effect. It is a normalized value dividing the difference between $V_{T,lin}$ in the linear region and $V_{T,sat}$ measured in the saturation region by V_{DD}. Figure 15 shows the DIBL of CORE MOSFET on the Y1-axis and IO MOSFET on the Y2-axis for the N-dose on the X-axis. The CORE MOSFET does not respond to nitrogen dose up to 1.3E15 cm^{-2} but drops off sharply above that. However, IO MOSFET does not respond even when N-dose increases to 2.5E15 cm^{-2}. This means that nitrogen implanted into the LDD contributes marginally to suppressing the short-channel effect in nanometer technology. This is probably because the short-channel effects have already been optimized through various other efforts.

D. EFFECT OF NITROGEN ON ID,SAT

We investigated the $I_{D,sat}$ response to N-dose. Figure 16 shows the $I_{D,sat}$ of HV MOSFET on the Y1-axis and IO MOSFET on the Y2-axis as a function of N-dose. Both $I_{D,sat}$ trends exhibit the same parabolic-like response. In the low dose range, $I_{D,sat}$ increases by 10% for IO MOSFET. However, $I_{D,sat}$ decreases after passing the inflection point around the N-dose of 1.0E15 cm^{-2}. These MOSFETs received the Well implantation under different process sequences and conditions. They also have different gate oxide thicknesses and lengths. Additionally, the LDD is processed on the same mask but opened after the spacer etch for HV MOSFET and before the spacer for IO MOSFET. Despite these differences, $I_{D,sat}$ show a similar parabolic-like response. This suggests that $I_{D,sat}$ could influenced by a few more mechanisms of nitrogen.

D.1. VERIFICATION OF CHANNEL LENGTH MODULATION

DIBL increases $I_{D,sat}$ but nitrogen did not affect the DIBL of IO MOSFET as discussed in Section III.C. Additionally,

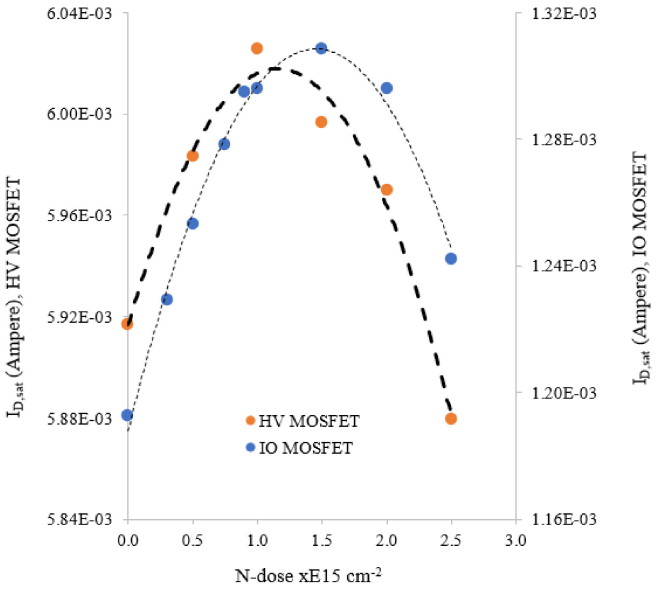

FIGURE 16. $I_{D,sat}$ exhibits a parabolic-like response to N-dose. HV MOSFET (Y1) V_D=V_G=5 Volt, IO MOSFET (Y2) V_D=V_G=2.5 Volt.

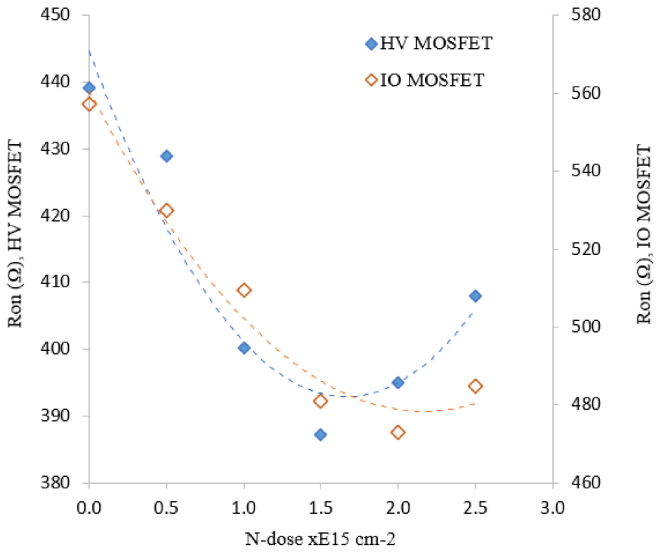

FIGURE 17. Ron trends of HV MOSFET (Y1) and IO MOSFET (Y2) for N-dose. Read at V_D=0.2 Volt, V_D=V_G=V_{DD}.

nitrogen is not expected to affect the DIBL of HV MOSFET, since the gate length is approximately 3 times longer than that of IO MOSFET. Another suspecting cause for the parabolic-like $I_{D,sat}$ is channel length modulation. As we discussed earlier, Cov decreases with a negative correlation with N-dose. That's because nitrogen suppressed the diffusion of LDD dopant on the silicon surface. Therefore, $I_{D,sat}$ should be decreased as N-dose increases. However, $I_{D,sat}$ increases in the low dose range and decreases only for doses higher than 1.0E15 cm^{-2}.

We analyzed Ron trends over N-dose to validate the channel length modulation. Figure 17 shows the Ron of the HV MOSFET on the Y1-axis and the IO MOSFET on the Y2-axis as a function of the N-dose on the X-axis, measured at V_D=0.2 Volt, V_D=V_G=V_{DD}. Ron is the series resistance of the channel and LDD. If Ron is dominated by channel resistance, it must increase because the channel distance from the drain to the source increases as N-dose increases. However, Ron decreases to ~15% for IO MOSFET and HV MOSFET shows a similar reduction of about ~12% despite having ~3 times longer gate length. Therefore, the Ron reduction does not come from the channel resistance but from LDD resistance.

D.2. INCREASES $I_{D,SAT}$ DUE TO ELECTRICAL ACTIVATION OF NITROGEN

Nitrogen is a commonly used species to produce N-type in high-voltage devices based on SiC or GaN semiconductors. However, it is known to be an electrically inactive species in silicon-based semiconductors. Therefore, it is widely used as an environmental gas in fabrication processes. In addition, it was reported that nitrogen implanted into intrinsic semiconductors has low solid solubility, so the probability of being substituted into the silicon lattice is less than 1% [14], [15].

However, when nitrogen is implanted into silicon with a high concentration of boron-doped, the solid solubility of nitrogen is enhanced because boron moves from a lattice to an interstitial, and the vacancy concentration increases [16]. All MOSFETs studied in this work were fabricated in heavily boron-doped P-type Wells. Therefore, the solid solubility of nitrogen can be increased with the help of boron, and the electrical activation of nitrogen can be improved.

We compared the $I_{D,sat}$ response to nitrogen with that of phosphorus co-implanted as an N-type dopant in the LDD of IO MOSFET. Figure 18 shows the $I_{D,sat}$ response for nitrogen and phosphorus on the Y-axis and their doses on the X-axis. Both show similar regression shapes. We extracted the relative activation ratio of nitrogen atoms to phosphorus using the equation obtained in the linear region as follows:

The equation (1) is for N-dose xE15 cm^{-2}, and (2) is for P-dose (Phosphorus dose) xE14 cm^{-2}.

$$I_{D,sat} = 1.06E - 4x + 0.0012 \quad (1)$$

$$I_{D,sat} = 1.50E - 4x + 0.0011 \quad (2)$$

Calculated the $I_{D,sat}$ ratio of nitrogen to phosphorus after normalizing the dose to 1.0E14 cm^{-2}.

$$(1.06E - 4/10)/1.50E - 4 * 100 = 7.1\% \quad (3)$$

Assuming that the phosphorus atoms are 100% activated and contribute to $I_{D,sat}$, output (3) indicates that approximately 7% of the implanted nitrogen atoms are electrically activated and contribute to $I_{D,sat}$.

The overall performance of IO MOSFET was compared considering the increase in $I_{D,sat}$ due to nitrogen activation, and the increase in $I_{D,off}$ due to the electric field. In the regression between $I_{D,off}$ and $I_{D,sat}$ in Figure 19, the

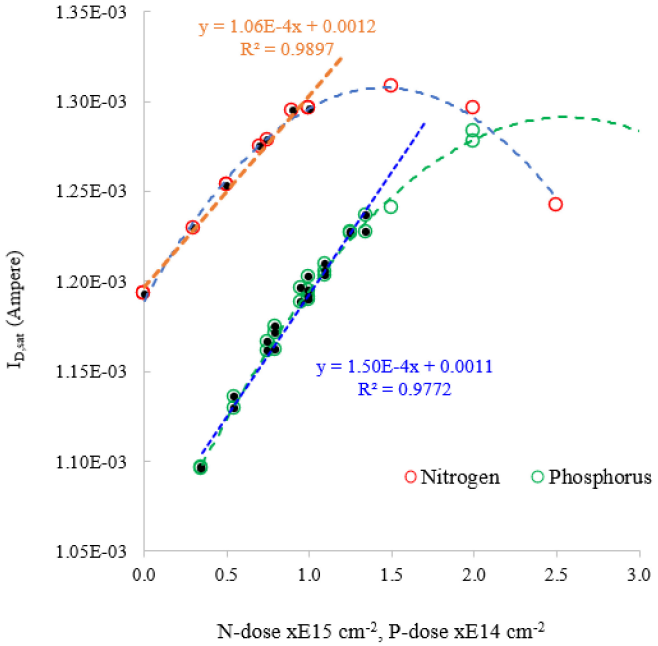

FIGURE 18. Regression curves of $I_{D,sat}$ for N-dose and P-dose show similar shapes. IO MOSFET. Read at V_D=V_G=2.5 Volt.

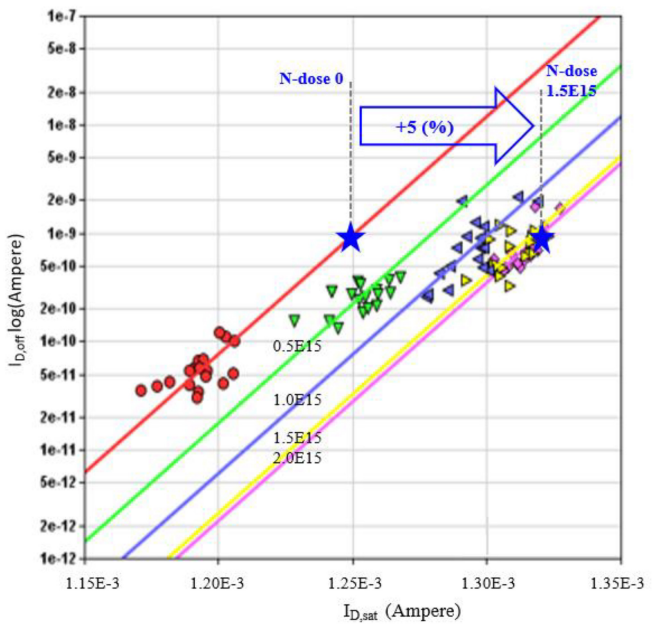

FIGURE 19. N-dose improves the performance of $I_{D,off}$ -$I_{D,sat}$ up to 5% at $I_{D,off}$ of 1E-9 Ampere. IO MOSFET.

maximum increment of $I_{D,sat}$ at the $I_{D,off}$ of 1E-9 Ampere is up to approximately 5% compared to N-dose 0.

D.3. DECREASES $I_{D,SAT}$ DUE TO ELECTRICAL DEACTIVATION OF PHOSPHORUS

$I_{D,sat}$ decreases when N-dose exceeds 1.0E15 cm^{-2}. According to the literature, phosphorus co-implanted with nitrogen shows a lower electrical activity than phosphorus alone because phosphorus readily combines chemically with

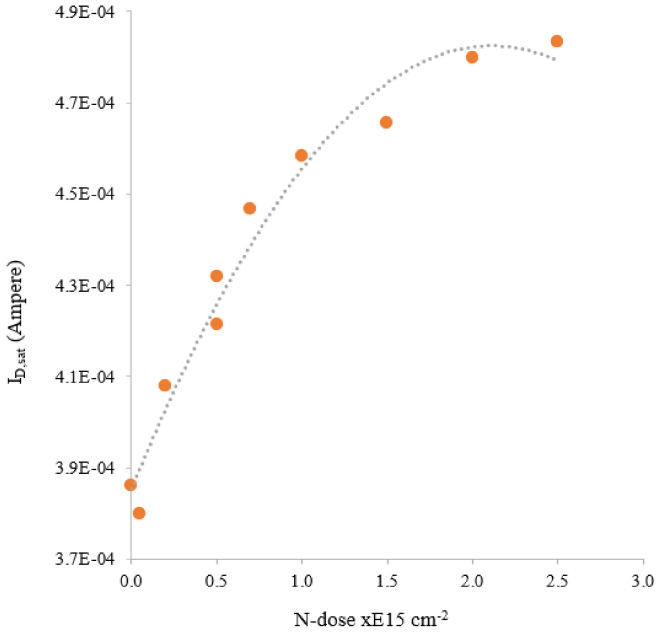

FIGURE 20. $I_{D,sat}$ of CORE MOSFET continues to increase as the N-dose increases up to 2.5E15 cm^{-2}. V_D=V_G=1.1 Volt.

nitrogen during annealing. The phosphorus atoms combined with nitrogen no longer act as donors [17]. Therefore, the increase in N-dose increases the probability of chemical bonding with phosphorus, resulting in $I_{D,sat}$ reduction. However, the boundary is unclear because phosphorus deactivation and nitrogen activation co-occur. The electrical activation of nitrogen increases as N-dose increases but reaches saturation at a given boron concentration. At the same time, the electrical deactivation of phosphorus increases and becomes the dominant effect from 1.0E15 cm^{-2}. As discussed earlier, the nitrogen concentration in the LDD bulk increases from the N-dose of 1.0E15 cm^{-2}, resulting in the tail-type $I_{D,off}$ and BV_{DSS}. Therefore, the probability of chemical bonding with nitrogen increases in the LDD bulk, and as a result, phosphorus deactivation becomes dominant from the N-dose of 1.0E15 cm^{-2}.

D.4. VERIFICATION OF ELECTRICAL ACTIVATION AND DEACTIVATION

We analyzed $I_{D,sat}$ trend for N-dose in CORE MOSFET (Fig. 20). It received a different LDD implantation scheme than IO and HV MOSFETs. Arsenic was implanted instead of phosphorus, and BF_2 was implanted with a high-degree tilt angle to suppress the short-channel effect. Nevertheless, $I_{D,sat}$ increases as N-dose increases. This indicates that electrical activation of nitrogen occurs also in CORE MOSFET. However, it does not exhibit an inflection point and decreasing trend even if it exceeds 1.0E15 cm^{-2}. That's because the chemical reactivity between nitrogen and arsenic is low. Therefore, electrical deactivation of arsenic by chemical bonding with nitrogen does not occur.

We investigated the chemical reactivity of phosphorus and arsenic toward nitrogen. As atomic numbers increase, chemical reactivity decreases. In group V of the periodic table, phosphorus is in period 3 and arsenic is in period 4. Therefore, arsenic has lower reactivity to nitrogen than phosphorus. According to the literature, nitrogen reacts well with phosphorus to form P_3N_5. However, the reaction of nitrogen and arsenic requires extremely high temperatures and pressures. Therefore, except for unstable and highly explosive compounds (e.g., $As(N_3)_3$, $As(N_3)_5$), covalent compounds composed of arsenic and nitrogen have not yet been reported [18].

IV. CONCLUSION

Nitrogen increases $I_{D,off}$ and reduces BV_{DSS} in HV MOSFET. When N-dose exceeds 1.0E15 cm^{-2}, HCI immunity degrades sharply. The short-channel effect of IO MOSFET is not affected by nitrogen. The benefit of nitrogen implantation in IO and HV MOSFETs is not much and may be eliminated. In this case, $I_{D,sat}$ decreases as the electrical activation of nitrogen disappears. Unlike IO and HV MOSFETs, nitrogen implanted into CORE MOSFET improves HCI immunity and increases $I_{D,sat}$ without an inflection point. For all MOSFETs, it is recommended that the nitrogen dosage not exceed 1.0E15 cm^{-2}.

Below is a summary of the results.

1) Nitrogen implanted into the LDD increases the electric field, as a result, BV_{DSS} decreases and $I_{D,off}$ increases.

2) Nitrogen enhances TED diffusion in the LDD bulk but suppresses it on the surface, forming a negative depletion curvature at the LDD edge and increasing the electric field.

3) When the N-dose exceeds 1.0E15 cm^{-2}, the nitrogen concentration in the LDD bulk increases and retards the recrystallization and leaving amorphous clusters.

4) Amorphous clusters form randomly steep junctions and increase the electric field. As a result, tail-type $I_{D,off}$ and BV_{DSS} occur.

5) Nitrogen improves the HCI immunity but degrades for IO and HV MOSFETs when N-dose exceeds 1.0E15 cm^{-2}.

6) The short-channel effect of IO MOSFET evaluated by DIBL is insensitive to nitrogen. However, CORE MOSFET is suppressed when the N-dose exceeds 1.3E15 cm^{-2}.

7) Nitrogen is electrically activated and reduces the Ron of the IO MOSFET and HV MOSFET by up to 15% and 12%, respectively.

8) Nitrogen increases the $I_{D,sat}$ of IO MOSFET by about 10% and improves $I_{D,off}$-$I_{D,sat}$ performance by up to 5%.

9) Assuming that LDD co-implanted phosphorus atoms are 100% activated and contribute to $I_{D,sat}$ of IO MOSFET, approximately 7% of the implanted nitrogen atoms are electrically activated and contribute to $I_{D,sat}$.

10) Phosphorus co-implanted into the LDD covalently binds to nitrogen and becomes electrically inactive. This effect becomes dominant when N-dose exceeds 1.0E15 cm^{-2}, and $I_{D,sat}$ decreases.

11) Covalent bonding between arsenic and nitrogen is difficult. Therefore, the $I_{D,sat}$ of CORE MOSFET with arsenic co-implanting does not decrease even if N-dose exceeds 1.0E15 cm^{-2}.

REFERENCES

[1] S. Nakashima, M. Takahashi, S. Nakayama, and T. Ohno, "Suppression of lateral transient enhanced dopant diffusion by nitrogen implantation and its application to fully depleted MOSFETs/SIMOX," in *Proc. Int. Conf. Ion Implant. Technol.*, vol. 1, Kyoto, Japan, 1999, pp. 122–125, doi: 10.1109/IIT.1999.812067.

[2] S. Shimizu et al., "Impact of surface proximity gettering and nitrided oxide side-wall spacer by nitrogen implantation on sub-quarter micron CMOS LDD FETs," in *Proc. Int. Electron Devices Meeting*, Washington, DC, USA, 1995, pp. 859–862, doi: 10.1109/IEDM.1995.499352.

[3] T.Kuroi et al., "Highly reliable 0.15um MOSFETs with surface proximity gettering (SPG) and nitride oxide spacer using nitrogen implantation," in *Symp. VLSI Technol. Tech. Dig.*, 1995, pp. 19–20, doi: 10.1109/VLSIT.1995.520839.

[4] K. Roy, S. Mukhopadhyay, and H. Mahmoodi-Meimand, "Leakage current mechanisms and leakage reduction techniques in deep-submicrometer CMOS circuits," *Proc. IEEE*, vol. 91, no. 2, pp. 305–327, Feb. 2003, doi: 10.1109/JPROC.2002.808156.

[5] B. Jayant Baliga, "Avalanche breakdown," in *Fundamentals of Power Semiconductor Devices*, 2nd ed. Raleigh, NC, USA: Springer, 2008, pp. 90–94.

[6] K. Y. Lim, X. Yu, and D. Yeo, "A study on gate-induced junction breakdown," in *Proc. 6th Int. Conf. Solid-State Integr. Circuit Technol.*, vol. 2, 2001, pp. 950–953, doi: 10.1109/ICSICT.2001.982052.

[7] B. Jayant Baliga, "Planar junction termination," in *Fundamentals of Power Semiconductor Devices*, 2nd ed. Raleigh, NC, USA: Springer, 2008, pp. 106–118.

[8] J. R. Shih, M. C. Chiang, H. C. Lin, R. Y. Shiue, Y. Peng, and J. T. Yue, "N-FET HCI reliability improvement by nitrogen interstitialization and its mechanism," in *Proc. IEEE Int. Rel. Phys. Symp.*, Dallas, TX, USA, 2002, pp. 272–277, doi: 10.1109/RELPHY.2002.996647.

[9] L. S. Adam, M. E. Law, and K. S. Jones, "Diffusion of implanted nitrogen in silicon," *J. Appl. Phys.*, vol. 87, no. 5, pp. 2282–2284, Mar. 2000. doi: 10.1063/1.372173.

[10] T. Tsunomura, A. Nishida, and T. Hiramoto, "Analysis of NMOS and PMOS difference in V_T variation with large-scale DMA-TEG," *IEEE Trans. Electron Devices*, vol. 56, no. 9, pp. 2073–2080, Sep. 2009, doi: 10.1109/TED.2009.202639.

[11] M. Orlowski, C. Mazure, and L. Mader, "Simulation of source/drain structures for submicron MOSFETs with and without preamorphization," in *Proc. 18th Eur. Solid State Device Res. Conf.*, Montpellier, France, 1988, pp. C4-557–C4-560, doi: 10.1051/jphyscol:19884117.

[12] O. Dokumaci, R. Kaplan, M. Khare, P. Ronsheim, and J. Burnham, "Diffusion and defect structure in nitrogen implanted silicon," *Mat. Res. Soc. Symp. Proc.*, vol. 669, pp. 1–6, Dec. 2001.

[13] W. Wong, A. Icel, and J. J. Liou, "A model for MOS failure prediction due to hot-carriers injection," in *Proc. IEEE Hong Kong Electron Devices Meeting*, Hong Kong, China, 1996, pp. 72–76, doi: 10.1109/HKEDM.1996.566313.

[14] P. V. Pavlov, E. I. Zorin, D. I. Tetelbaum, and A. F. Khokhlov, "Nitrogen as dopant in silicon and germanium," *Physica Status Solidi (a)*, vol. 35, no. 1, pp. 11–36, 1976.

[15] B. Guan et al., "Nanoscle nitrogen doping in silicon by self–assembled monolayers," *Sci. Rep.*, vol. 5, Jul. 2015, Art. no. 12641, [Online]. Available: https://www.nature.com/scientificreports

[16] D. I. Tetelbaum, E. I. Zorin, and N. V. Lisenkova, "Anomalous solubility of implanted nitrogen in heavily boron-doped silicon," *Semiconductors*, vol. 38, no. 7, pp. 775–777, 2004.

[17] R.-D. Chang and C.-H. Lin, "Deactivation of phosphorus in silicon due to implanted nitrogen," *Phys. Status Solidi C*, vol. 11, no. 1, pp. 24–27, doi: 10.1002/pssc.201300131.

[18] M. Ceppateilli, D. Scelta, M. Serrano-Ruiz, K. Dziubek, M. Morana, and V. Svutlyk, "Single-bonded cubic AsN from high-pressure and high-temperature chemical reactivity of arsenic and nitrogen," *Angew. Chem. Int. Ed. Engl.*, vol. 61, no. 6, Feb. 2022, Art. no. e202114191, doi: 10.1002/anie.202114191.